

Preparation of antimony-doped nanoparticles by hydrothermal method^①

JIANG Ming-xi(江名喜)¹, YANG Tian-zu(杨天足)¹, GU Ying-ying(古映莹)¹,
DU Zuo-juan(杜作娟)¹, LIU Jian-ling(刘建玲)²

(1. School of Metallurgical Science and Engineering,
Central South University, Changsha 410083, China;

2. College of Chemistry and Chemical Engineering, Hunan University, Changsha 410082, China)

Abstract: Antimony-doped tin oxide (ATO) nanoparticles were prepared by the mild hydrothermal method at 200 °C using sodium stannate, antimony oxide, sodium hydroxide and sulfuric acid as the starting materials. The doped powders were examined by differential thermal analysis (DTA), X-ray diffractometry (XRD) and transmission electron microscopy (TEM). The doping levels of antimony were determined by volumetric method and iodometry. The results show that antimony is incorporated into the crystal lattice of tin oxide and the doping levels of antimony in the resulting powders are 2.4%, 4.3% and 5.1% (molar fraction). The mean particle size of ATO nanoparticles is in the range of 25–30 nm. The effects of antimony doping level on the crystalline size and crystallinity were also discussed.

Key words: hydrothermal process; nanoparticle; antimony; doping; tin oxide

CLC number: TF 123

Document code: A

1 INTRODUCTION

Tin oxide is an n-type semiconductor with a wide band gap of about 3.6 eV and with the highest carrier mobility among the oxides^[1]. Due to the advantageous electrical and optical properties, SnO₂ ultrafine powders have been widely used for technical applications, such as gas sensors, burglar alarms and catalyst^[2]. In order to improve the electrical and optical properties further, the doped tin oxide has been extensively investigated, especially for antimony and fluorine-doped tin oxide. The introduction of some amount of antimony into the crystal lattice of tin oxide can greatly increase the electronic conductivity and depress the growth of particles, while the optical property is not devastated. Antimony-doped tin oxide is widely used as the high-performance materials for the production of transparent electrodes^[3, 4], energy storage device^[5, 6], printed displays, liquid crystal displays, electrochromic displays^[7-9], heating elements in aircraft, special furnaces and luminescent lamps etc^[10-12].

At present, the main methods used for the synthesis of ATO nanometer powders are as follows: the solid-state reaction method^[13], the sol-gel method^[7], the coprecipitation method^[14-17] and the hydrothermal method^[18-20]. At the high reaction temperature for the solid-state method, the re-

sulting powders are inhomogeneous distribution of the doped elements, large particle size and easiness to introduce other impurities, so it is rarely used for the preparation of ATO nanoparticles. For the coprecipitation method, a post-calcination at over 500 °C is required and this causes a large particle size and heavy agglomeration. Among the investigations on the preparation of ATO nanoparticles, the chlorides of tin and antimony, such as SnCl₄, SnCl₂, SbCl₃ and SbCl₅ are commonly employed as the starting materials. Chlorine ions are easily adsorbed on tin hydroxide and very difficult to be washed off. The residual chlorine ions are usually eliminated by calcinations at high temperature, which leads to the volatilization of antimony and tin, affects the surface and electrical properties of powders, introduces a random n-type doping in the material, and causes agglomeration among particles and difficulty for sintering^[19]. So the starting materials free from chlorides should be considered for the preparation of ATO powders. The ATO powders with narrow particle size distribution, low coacervation, high purity and fine crystallization can be synthesized directly by the hydrothermal method without the necessity of calcination.

In this paper, sodium stannate, antimony oxide, sodium hydroxide and sulfuric acid are used as the starting materials for the preparation of ATO nanoparticles by the mild hydrothermal method.

① **Foundation item:** Project(2001BA901A09) supported by the Key Program of Scientific and Technology Action of West China Development

Received date: 2004-10-28; **Accepted date:** 2005-01-07

Correspondence: JIANG Ming-xi, PhD candidate; Tel: +86-731-8836791; E-mail: jmingxi@yahoo.com

2 EXPERIMENTAL

2.1 Preparation process

Given amounts of antimony oxide and sodium stannate were dissolved in 100 mL sodium hydroxide solution of 200 g/L and 100 mL de-ionized water respectively. NaSbO_2 solution and Na_2SnO_3 solution were mixed proportionally depending on the antimony doping level required. 35 mL of the mixed solution was then dropped from a burette into a 100 mL conical flask with 5 mL de-ionized water in concurrent addition of 33% (volume fraction) sulfuric acid from the other burette, which was intensively agitated and heated at 60 °C by a magnetic stirrer.

The final pH value of the solution was kept at 1.5 for getting a light yellow suspensions of ATO precursor, and then the precursor was poured into a 100 mL polytetrafluoroethylene-lined autoclave and heated at 200 °C for 8 h. After that, the autoclave was quenched by tap water to the room temperature. The blue color powders were isolated by centrifugation, washed with de-ionized water until no SO_4^{2-} could be detected (by 0.1 mol/L BaCl_2 solution). The final powders were rinsed three times with absolute alcohol and dried at 80 °C, then ground in an agate mortar. The preparation process of ATO nanoparticles is shown in Fig. 1.

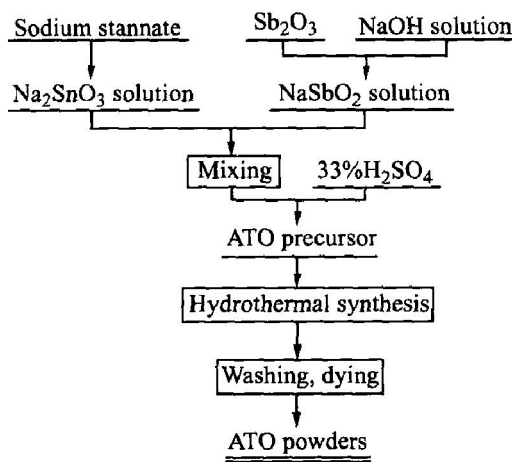


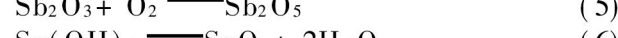
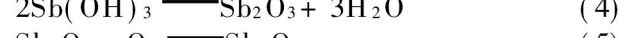
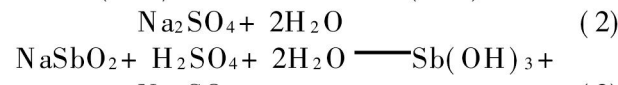
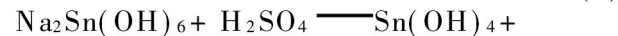
Fig. 1 Flowsheet for preparation of ATO nanoparticles by hydrothermal method

2.2 Characterization

The ATO powders with different doping levels were characterized by X-ray diffractometry (XRD), transmission electron microscopy (TEM) and differential thermal analysis (DTA). The crystal sizes, lattice parameters and lattice distortion rates of the powders were calculated.

3 RESULTS AND DISCUSSION

The reactions during the preparation of antimony-doped tin oxide are summarized as follows.



The antimony doping levels of the samples were determined by volumetric method and iodometry. The doping levels for sample A, B and C are 5.1%, 4.3% and 2.4% (molar fraction), respectively.

Fig. 2 shows the DTA curves of the samples. There are neither endothermic peaks nor exothermic peaks found in the DTA curves. This indicates that neither adsorptive water nor bonding water exist in the powders and the dehydration of the ATO precursor is carried out completely at 200 °C. It also illustrates that the crystallographic form of the powders is very stable as there is no changes till about 900 °C.

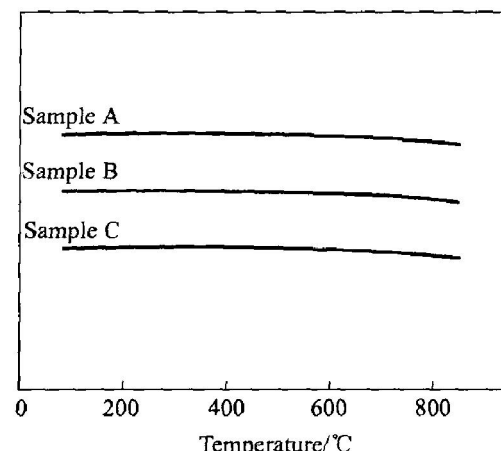


Fig. 2 DTA curves of samples

The X-ray diffraction patterns of ATO nanoparticles are shown in Fig. 3. The X-ray diffraction peaks of tin oxide are in good agreement with those of the tetragonal phase of rutile of tin oxide, without additional peaks belonging to other phases such as Sb_2O_3 . The X-ray diffraction patterns indicate that all the antimony ions have been incorporated into the crystal lattice of tin oxide. The diffraction peaks are intensively broadened and the full peak width increases with the increase of the antimony doping level. The crystalline size of the powders is very small and decreases with the increase of the antimony doping level, while the crystallinity of ATO powders becomes low with the rising of antimony doping content. The mean crystalline size of the particles can be calculated from the [110] crystal planes by the Scherrer formula^[21].

$$D_{hkl} = (K\lambda)/(10\beta \cos \theta_B) \quad (7)$$

The results are listed in Table 1.

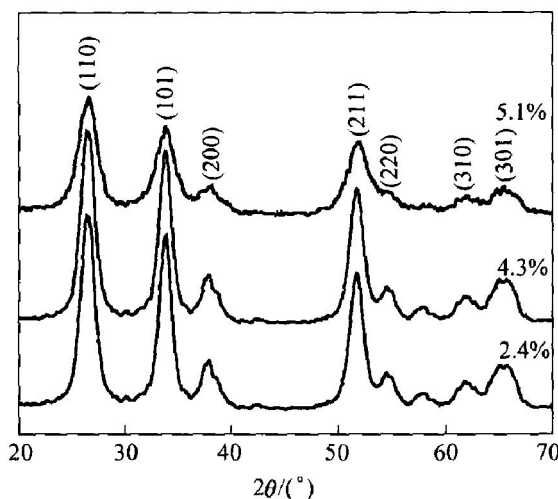


Fig. 3 X-ray diffraction patterns of ATO nanoparticles synthesized at various antimony doping levels

(a) —Sample A; (b) —Sample B; (c) —Sample C

Table 1 Mean crystalline size and unit cell parameters of ATO nanoparticles

Sample	Antimony doping level (molar fraction) / %	Mean crystalline size/ nm	
A	5.1	4.8	
B	4.3	6.3	
C	2.4	7.1	
Sample	Cell parameters		Cell volume/ 10 ⁻³ nm ³
	<i>a</i> / nm	<i>c</i> / nm	
A	0.4711	0.3197	70.96
B	0.4678	0.3220	70.46
C	0.4676	0.3211	70.21

The unit cell parameters, σ axis, σ axis lengths, cell volume and the lattice distortion rate of tin oxide as the function of antimony doping level can also be calculated according to the following equations^[21, 22]:

$$D_{hkl} = 1/\sqrt{(h^2 + k^2)/a^2 + l^2/c^2} \quad (8)$$

$$a^2 = \{[(h_2^2 + k_2^2)l_1^2 - (h_1^2 + k_1^2)l_2^2]/(l_1^2d_1^2 - l_2^2d_2^2)\} \quad (9)$$

$$c^2 = l_1^2d_1^2/[1 - (h_1^2 + k_1^2)d_1](1/a^2) \quad (10)$$

$$(2\omega)^2 \cos^2 \theta = 4/\pi^2 (\chi D_{hkl})^2 + 32\langle \varepsilon^2 \rangle_{hkl} \sin^2 \theta \quad (11)$$

The calculated results are listed in Table 1 and Table 2. The cell volume increases with the increase of the antimony doping level. The ionic radii of Sn^{4+} , Sb^{5+} and Sb^{3+} are 0.071 nm, 0.062 nm and 0.092 nm respectively. When doping, if antimony is incorporated into the lattice of tin oxide to substitute Sn^{4+} in the form of Sb^{5+} , the unit cell of ATO nanoparticles would shrink for the ionic radius of Sb^{5+} is smaller than that of Sn^{4+} and it would expand when antimony enter into the lattice of tin oxide in the form of Sb^{3+} for the ionic radius of Sb^{3+} is larger than that of Sn^{4+} . It is reported^[7]

that at the low doing level, most of the antimony ions exist in the form of Sb^{5+} , thus the volume of unit cell will be smaller than that of pure tin oxide. With the Sb doping level rising, part of the antimony ions enter into the lattice in the form of Sb^{3+} and the $\text{Sb}^{3+}/\text{Sb}^{5+}$ ratio will increase with the antimony doping level, so the cell volume of tin oxide will expand accordingly. The volume of unit cell becomes larger than that of pure tin oxide when the antimony doping level reaches a certain degree. In the doping levels in this paper, the cell volumes of all the samples are smaller than that of pure tin oxide (71.52×10^{-3} nm³)^[9]. This illustrates that the antimony ions doped mainly exist in the form of Sb^{5+} . The lattice distortion rate increases with the increase of antimony doping level. This is why the crystallinity of the ATO powders becomes lower as the doping level rises.

Figs. 4(a) and (b) show the TEM images of

Table 2 Lattice distortion rate($\langle \varepsilon^2 \rangle_{110}^{1/2}/10^{-3}$) of samples

Sample A	Sample B	Sample C
4.3	3.5	3.1

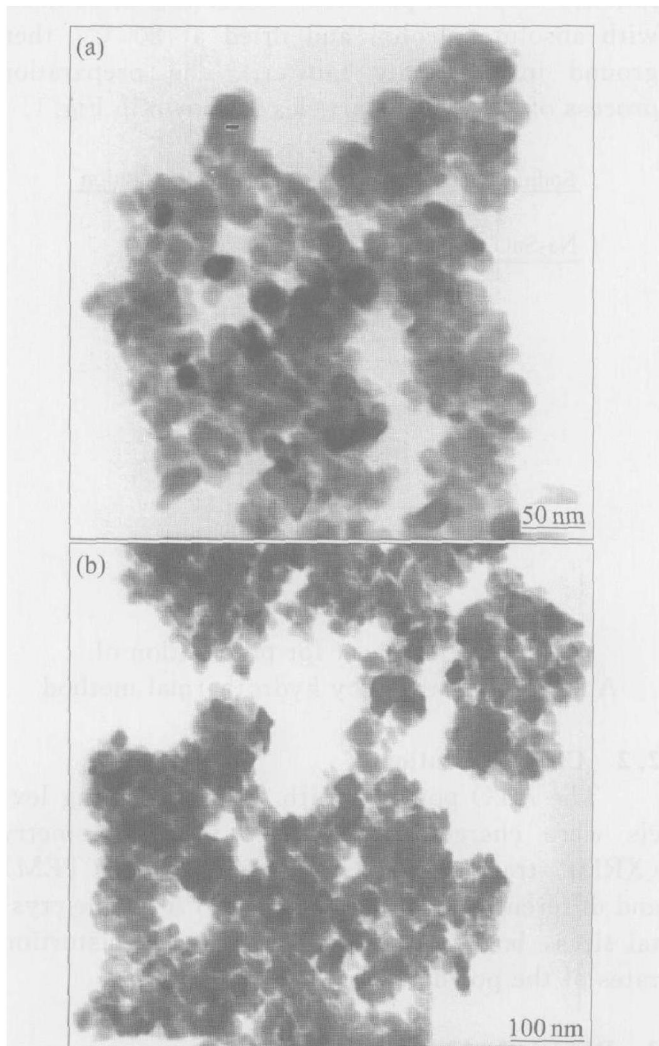


Fig. 4 TEM images of ATO nanoparticles synthesized at 200 °C
(a) —Sample A; (b) —Sample B

the synthesized ATO nanoparticles. The average particle sizes of samples A and B are about 25 nm and 30 nm respectively.

4 CONCLUSIONS

ATO powders with the mean particle size ranging 25 – 30 nm have been successfully prepared by the mild hydrothermal method free from chloride. Sulfuric acid was used as the precipitating agent. The effects of antimony doping level on the crystalline size and the crystallinity of ATO powders are also investigated. The experimental results show that the crystalline size decreases and the crystallinity becomes lower with the increase of Sb doping level.

REFERENCES

- [1] Szcuklo D, Werner J, Oswald S, et al. XPS investigations of surface segregation of doping elements in SnO_2 [J]. Applied Surface Science, 2001, 179: 301 – 302.
- [2] GUO Yuzhong, WANG Jianhua, HUANG Ru'an. Electrical and optical properties of transparent and conductive Sb-doped SnO_2 films [J]. Journal of Inorganic Materials, 2002, 17(1): 131 – 138. (in Chinese)
- [3] Gržeta B, Tkalcic E, Goebbert C, et al. Structure studies of nanocrystallite SnO_2 doped with antimony: XRD and Mossbauer spectroscopy [J]. Physics and Chemistry of Solids, 2002, 63: 765 – 772.
- [4] Garima J, Kumar R. Electrical and optical properties of tin oxide and antimony doped tin oxide film [J]. Optical Materials, 2004, 26: 27 – 31.
- [5] Terrier C, Chatelon J P, Roger J A. Electrical and optical properties of Sb: SnO_2 thin films obtained by the sol-gel method [J]. Thin Solid Films, 1997, 295: 95 – 100.
- [6] Kim K S, Yoon S Y, Lee W J, et al. Surface morphologies and electrical properties of antimony-doped tin oxide films deposited by plasma-enhanced chemical vapor deposition [J]. Surface and Coatings Technology, 2001, 138: 229 – 236.
- [7] MIAO Hongyan, DING Changsheng, LUO Hongjie. Antimony doped tin dioxide nanometer powders prepared by the hydrothermal method [J]. Microelectronic Engineering, 2003, 66: 142 – 146.
- [8] WEI Zhixian, FAN Wen-hao, CHENG Zhunhua, et al. Preparation of Sb-doped SnO_2 ultrafine powder via oxidative coprecipitation [J]. The Chinese Journal of Process Engineering, 2002, 2(2): 151 – 155. (in Chinese)
- [9] ZHANG Jianrong, GU Da, YANG Yurxia. Crystal and electrical behavior of antimony doped SnO_2 nanoparticles [J]. Chinese Journal of Applied Chemistry, 2002, 19(6): 552 – 555. (in Chinese)
- [10] ZHANG Jianrong, GAO Lian. Synthesis of antimony-doped tin oxide(ATO) nanoparticles [J]. Inorganic Chemistry Communications, 2004, 7: 91 – 97.
- [11] ZHEN Zang-Shen, DONG Jie, ZHANG Ping. Preparation of antimony doped tin oxide based ceramic conductive film [J]. Journal of Hebei Institute of Technology, 2001, 23(4): 73 – 77. (in Chinese)
- [12] QIN Chang-yong, LUO MeiFang, GU Hong-Chen, et al. Effect of preparation process on particle size distribution of ultrafine ATO powders [J]. The Chinese Journal of East China University of Science and Technology, 2001, 27(3): 261 – 264. (in Chinese)
- [13] Volta J V, Bussiere P, Coudurier G, et al. Tin-antimony mixed oxides: tentative active site identification [J]. Appl Catal, 1985, 16(3): 315 – 318.
- [14] Coleman J P, Freeman J J, Madhukar P, et al. Electrochronism of nanoparticulate doped metal oxides: optical and material properties [J]. Displays, 1999, 20: 145 – 154.
- [15] YANG Huaming, HU Yuehua, QIU Guanzhou. Preparation of antimony-doped SnO_2 nanocrystallites [J]. Material Research Bulletin, 2002, 37: 2453 – 2458.
- [16] ZHANG Jianrong, GU Da. Wet-chemical synthesis of ATO nanoparticles [J]. Journal of Function Materials, 2002, 33(3): 300 – 302.
- [17] LI Qinshan, ZHANG Jinzhao. Influence of co-precipitation conditions on the particle size and conductive properties of Sb/ SnO_2 nano-sized powder [J]. Chinese Journal of Applied Chemistry, 2002, 19(2): 163 – 167.
- [18] Goebbert C, Nonninger R, Aegeiter M A, et al. Wet chemical deposition of ATO and ITO coating using crystalline nanoparticles redispersable in solutions [J]. Thin Solid Films, 1999, 351: 79 – 84.
- [19] ZHANG Jianrong, GAO Lian. Hydrothermal synthesis of antimony-doped tin oxide (ATO) nanoparticles and electrical properties [J]. Acta Chimica Sinica, 2003, 61(10): 1679 – 1681. (in Chinese)
- [20] ZHANG Jianrong, GAO Lian. Synthesis and characterization of antimony-doped tin oxide nanoparticles by the new hydrothermal method [J]. Material Science Communication, 2004, 87: 10 – 12.
- [21] YANG Naru. Testing Methods of Inorganic Nonmetals Materials [M]. Wuhan University of Technology Press, 1990. 91. (in Chinese)
- [22] LI Quan, ZENG Guang-Fu, XI Shiquan. Heat treatment and microstructure of nanosized stannic oxide powders [J]. Journal of Applied Chemistry, 1995, 12(2): 68. (in Chinese).

(Edited by YANG Bing)